

# Steady-State Pitch Angle Distributions of Radiation Belt Electrons Subject to Multiple Bounces

Julia Claxton (she/they), Robert Marshall – University of Colorado, Boulder

## Motivation

When particles in the loss cone collide with the atmosphere, a fraction of the incoming particles are scattered back along the field line in a new pitch angle and energy configuration. These backscattered particles form a new distribution observed mostly in the anti-loss cone. Since backscattered populations tend to reside in the anti-loss cone, they reach the magnetically conjugate atmosphere and undergo another collision and backscattering process. This 2nd-bounce population then mirrors back to the original hemisphere in the loss cone, continuing in this pattern until the distribution reaches a steady state.

These multibounce effects have not been considered in studies of EPP. This work uses the G4EPP library<sup>1</sup> based on the Geant4 physics engine<sup>2</sup> to perform multi-bounce EPP simulations and quantify the impact of multibounce effects on in-situ measured electron distributions.

## EPP Model

This project uses an adaptation of the G4EPP library developed by Grant Berland<sup>1</sup> to simulate EPP backscatter. The G4EPP library provides lookup tables with backscattered electron momenta for a grid of monoenergetic, mono-pitch angle input electron beams. The backscatter lookup tables were generated via simulation in Geant4<sup>2</sup>. Arbitrary energy-pitch angle distributions can be constructed via a weighted sum of the backscatter contributions of these input beams.

### Model Validation – ELFIN

- Electron Losses and Fields Investigation (ELFIN)<sup>3</sup>
- 3 years of data (2019-2022) over 2 satellites
  - Provided pitch angle & energy resolved electron data
  - ~22.5° angular resolution, energy range from 50 keV to 7200 keV (log-spaced bins)
  - LEO ⇒ Resolvable loss cone ( $\alpha_{LC} \approx 67^\circ$ )

### 1. Event Detection

For each timestep in ELFIN data, we calculate a precipitation score as follows:

1. Zero out readings with  $J_{prec}/J_{trap} < 10^{-75}$
2. Remove readings with fewer than 3 non-zero pixel neighbours
3. Sum vertically (along energy) for score
4. Set score to the highest value of score in the nearest 4 timesteps in both directions.

We then detect an event where the precipitation score exceeds a threshold of 2. This process is shown in Figure 1.

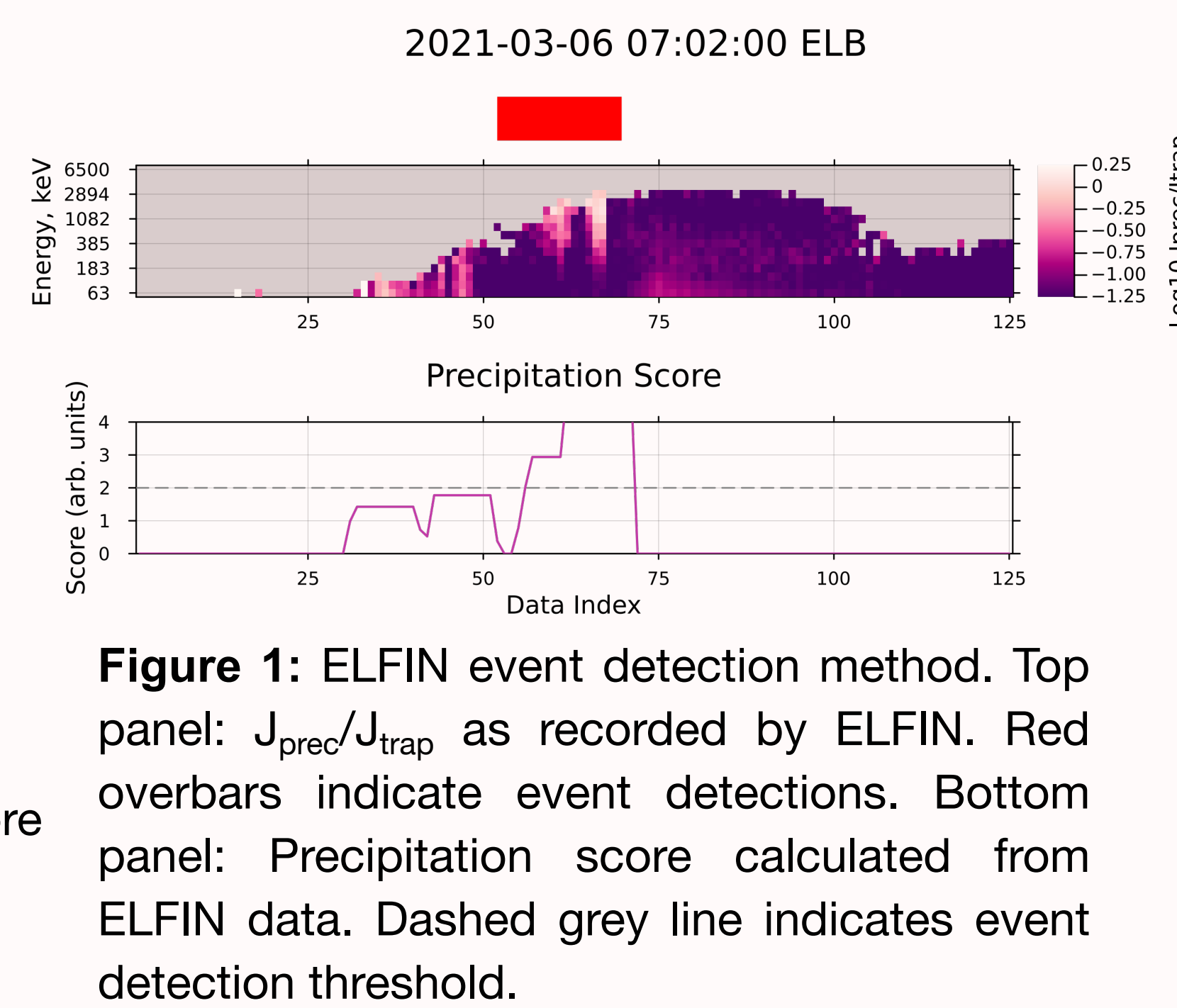


**Figure 1:** ELFIN event detection method. Top panel:  $J_{prec}/J_{trap}$  as recorded by ELFIN. Red overbars indicate event detections. Bottom panel: Precipitation score calculated from ELFIN data. Dashed grey line indicates event detection threshold.

### 2. Event Fitting

Each detected event is simulated in G4EPP as follows:

1. Integrate ELFIN flux over time range of event for directional differential fluence
2. For each energy/pitch angle ELFIN records, integrate directional differential fluence for total number of electrons recorded
3. Locate nearest precalculated beam in G4EPP and add number of electrons from step 2 to it
4. Weight backscatter lookup tables by number of electrons each beam has and look up backscatter

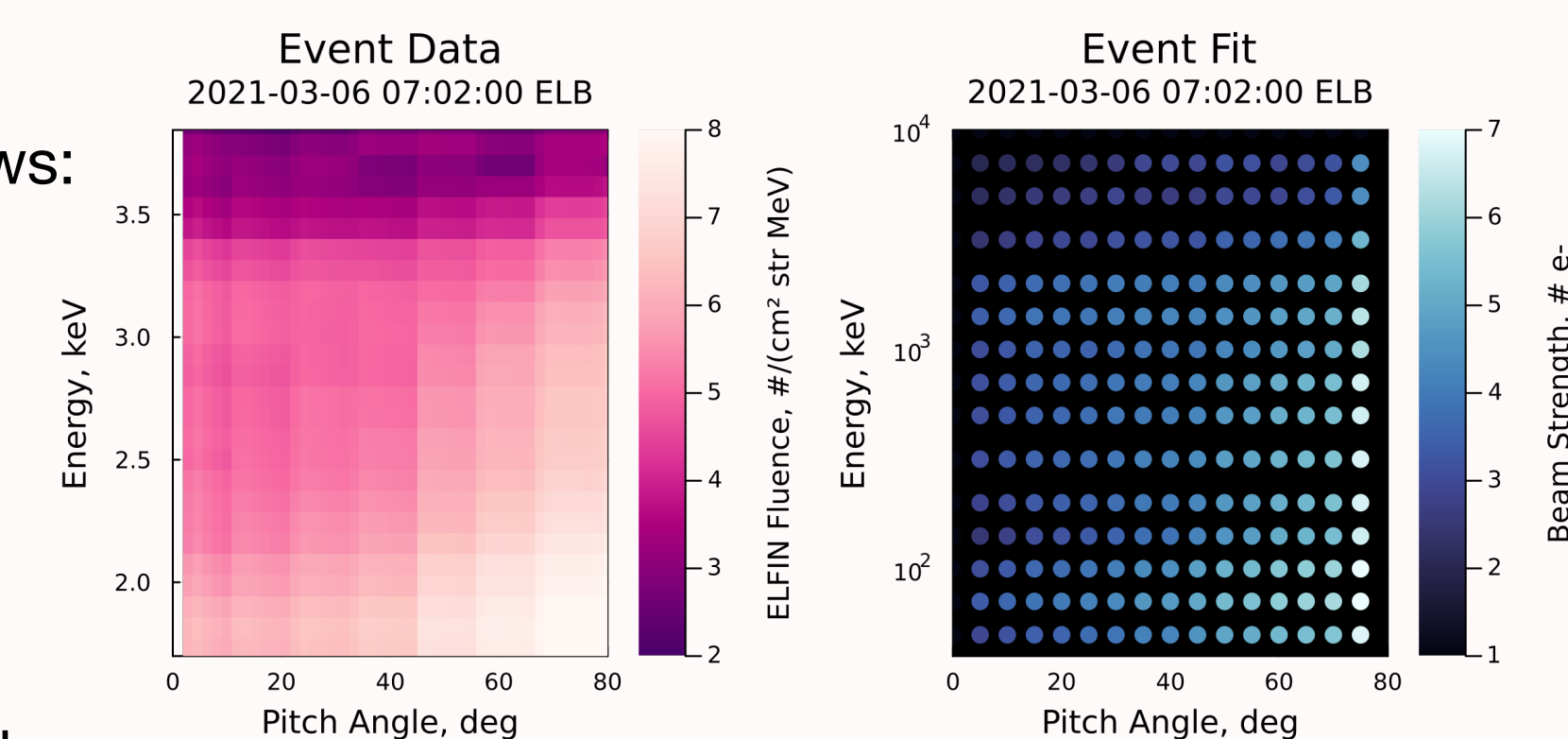


**Figure 2:** Fitting an ELFIN event to the G4EPP beams. Left panel: ELFIN fluence for event detected in Figure 1. Right panel: G4EPP beam strengths corresponding to the left panel fluence.

### 3. Calculate Residuals

We calculate the following three statistics for both the ELFIN data and the simulated events.

1. **Backscattered Energy:** Total energy in the anti loss cone.
2. **Backscattered Number:** Total number of electrons in the anti loss cone.
3. **Flux Distribution:** Differential directional number flux at each energy & pitch angle ELFIN records.

For every simulated event, each statistic is calculated for the data and the simulation. A residual is obtained by dividing the statistic's simulation-based value by its data-based (truth) value. The distribution of these residuals is shown in the "Model Accuracy" section.

## Model Accuracy

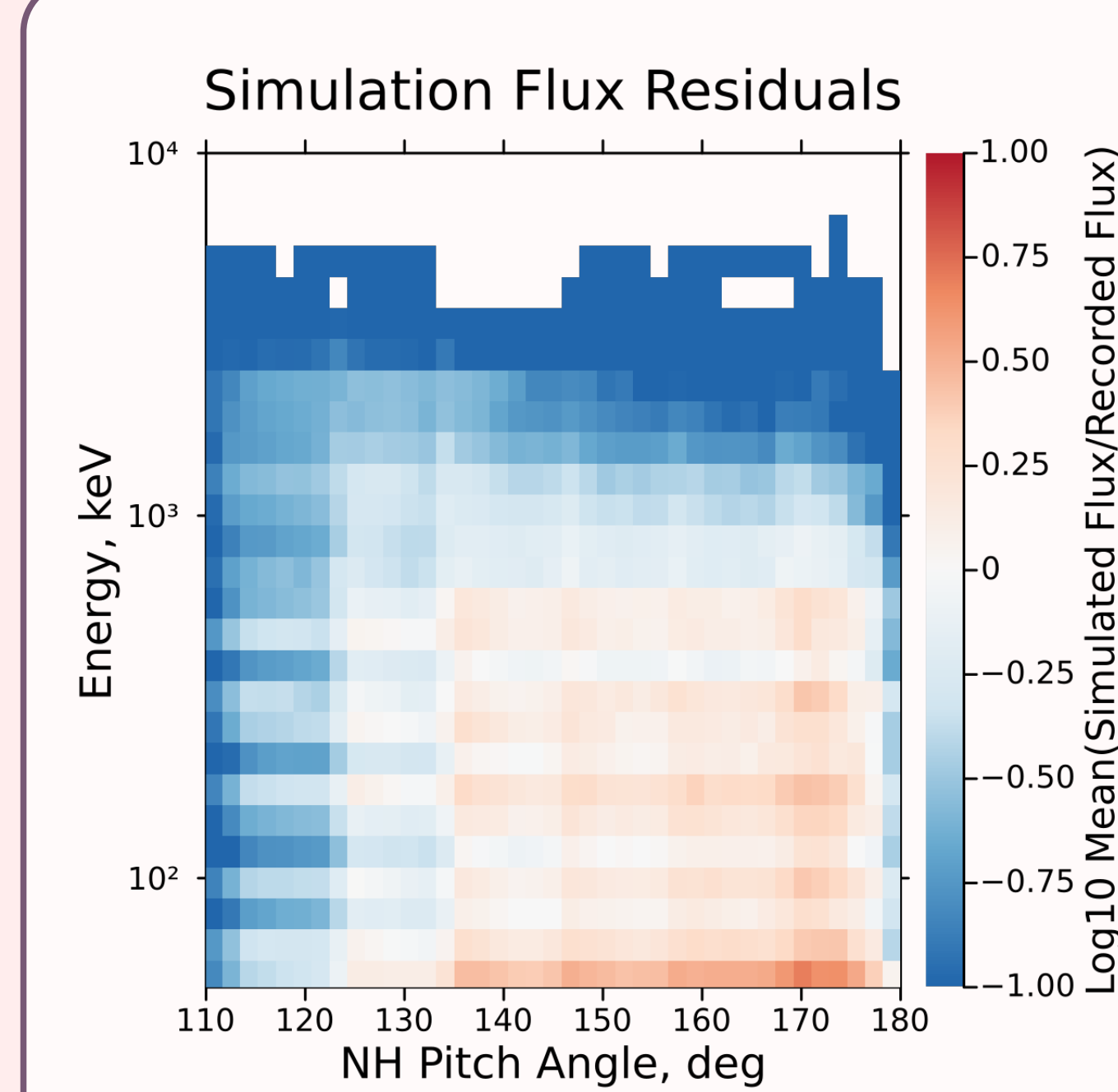


**Figure 3:** Average simulated electron number flux divided by recorded flux for ELFIN EPP events simulated with G4EPP as a function of pitch angle and energy.

Figure 3 (left) shows G4EPP's tendency to "flatten" backscattered energy/pitch angle distributions, by underestimating backscattered fluxes in the grazing region where fluxes are high, and overestimating fluxes deep in the anti loss cone where fluxes are low. In general, fluxes are correct within an order of magnitude and are often correct with a factor of  $10^{\pm 5}$ . Figure 4 (below) shows that while G4EPP in general underestimates total backscattered energy by up to nearly 2 orders of magnitude, it predicts total backscatter number relatively accurately. As such, we will only consider statistics based on number units rather than energy units for this work.

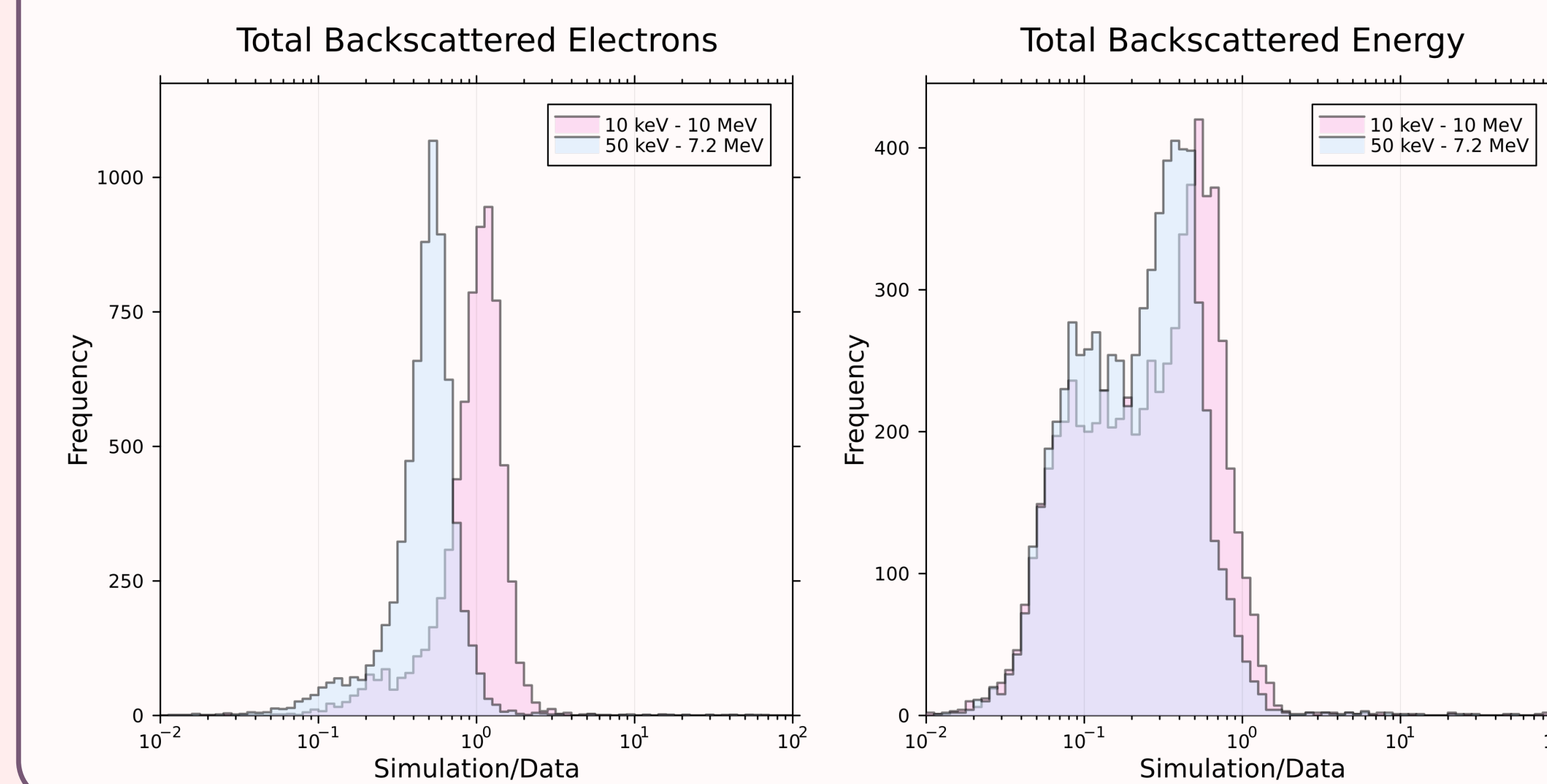


**Figure 4:** Total number of electrons in the anti loss cone (left) and total energy in the anti loss cone (right) for G4EPP simulations of ELFIN events. G4EPP has a larger energy range than ELFIN. Residuals over the G4EPP energy range are overlaid with residuals over the ELFIN energy range.

## Simulated Multibounce Effects

With the G4EPP model validated, we then used the ELFIN data as a source of realistic pitch angle/energy distributions, providing realistic simulation inputs ranging over a variety magnetospheric locations and activity levels. Each ELFIN EPP event detected was used as an input distribution to measure the impacts of multibounce effects. We quantify the impact of multibounce effects on a PAD using a metric called the 'multibounce fraction', defined as:

$$\text{Multibounce Fraction} = \frac{\sum \# \text{ electrons with } > 2 \text{ bounces}}{\text{Total } \# \text{ e-}}$$

The multibounce fraction tells us what fraction of the electrons measured in a PAD are due to the effects of multiple bounces – i.e what fraction of the distribution consists of double- (or triple-, quad-, etc.) counted electrons. The distribution of multibounce fractions for the loss cone and anti loss cone, derived from ELFIN's measured pitch angle/energy distributions, is shown below (Figure 5).

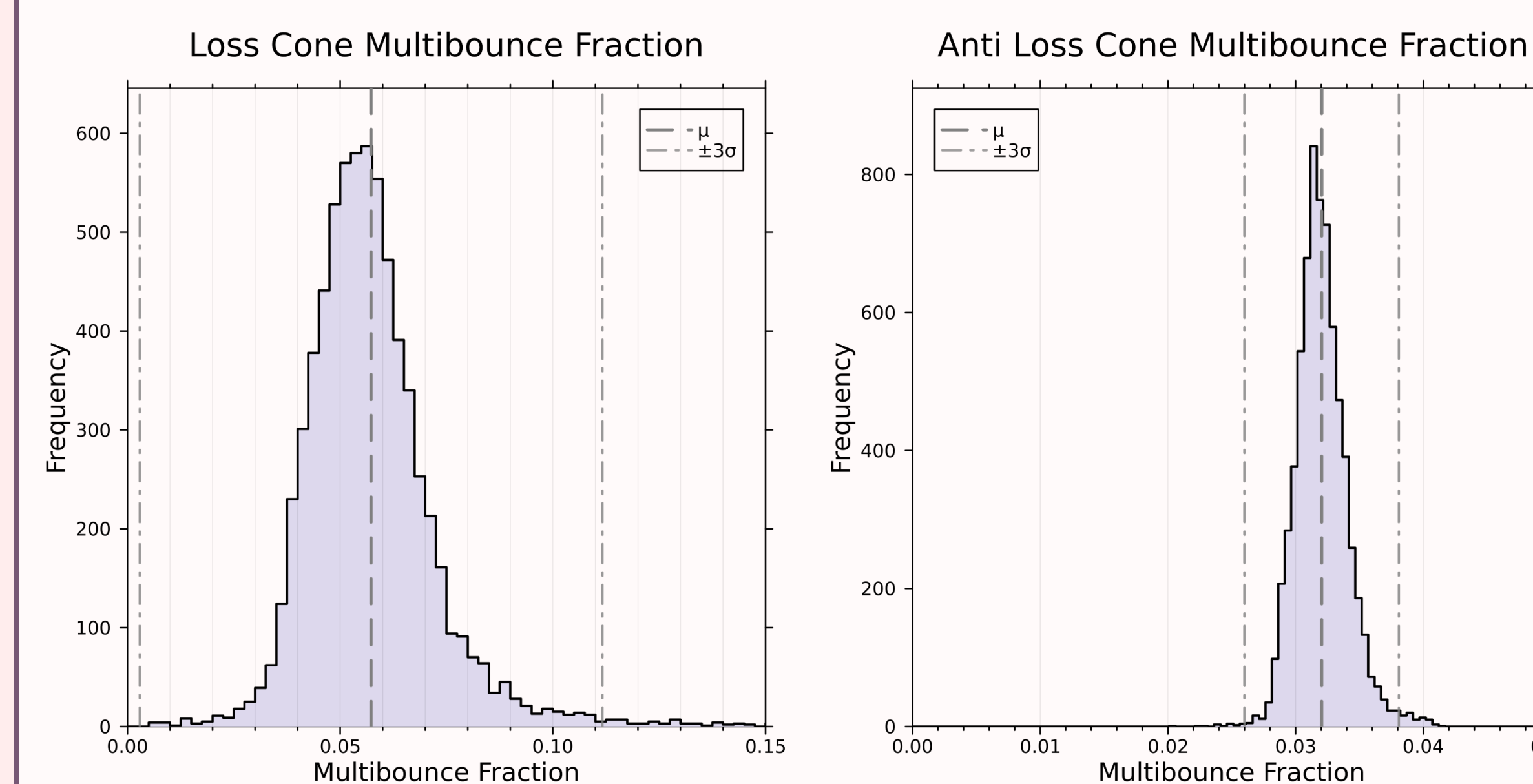


**Figure 5:** Distribution of multibounce fractions by number for the loss cone and anti loss cone for ELFIN-derived pitch angle/energy distributions.

Figure 5 shows that for realistic input distributions, we can expect up to ~10% of electrons measured in the loss cone to be due to multibounce effects, and up to ~4% of the anti loss cone to be due to multibounce effects. Depending on detector geometry and resolution, this can have varying impacts on the measured flux magnitude.

## Backscatter Statistics

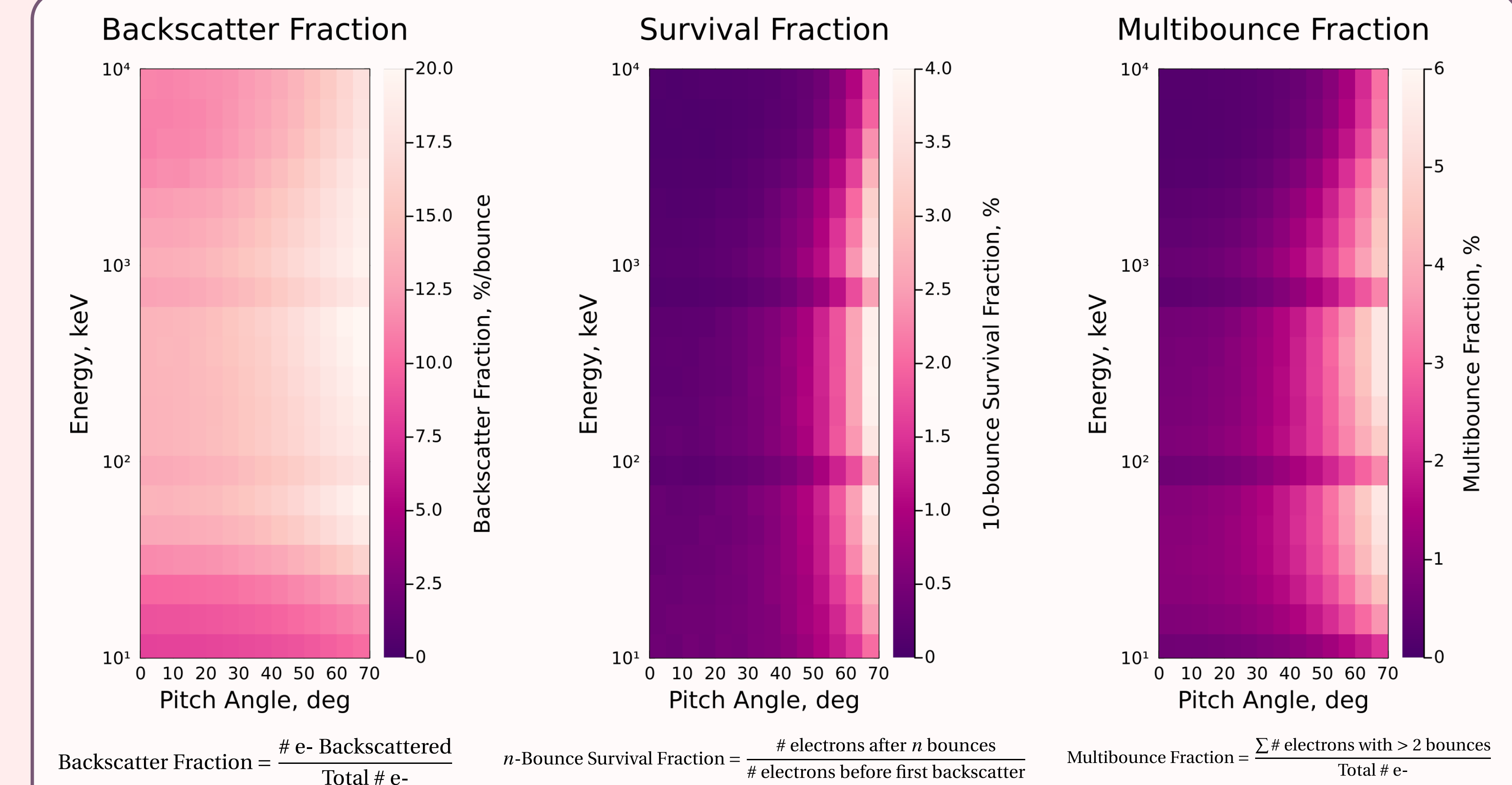


**Figure 6:** Charts showing how backscatter fraction, survival fraction, and multibounce fraction vary with pitch angle and energy. Each pixel represents a monoenergetic, mono-pitch angle input. The loss cone for this simulation begins around 67°. The dark bands at ~100 keV and ~800 keV are simulation artifacts and currently under investigation.

Figure 6 (above) shows a variety of backscatter statistics as a function of pitch angle and energy. In general, we see that grazing electrons (i.e. near the loss cone edge) experience fewer atmospheric effects, with high backscatter rates, survival rates, and multibounce effects. We also find that there is a 'sweet spot' in energy where particles experience the fewest atmospheric effects, from about 20 keV to 1 MeV. Particles above this energy penetrate too deep into the atmosphere to backscatter, while particles below this energy lose too much of their total energy in a single collision to escape the atmosphere.

## Conclusions

1. The G4EPP library provides backscatter lookup tables that are generally accurate for number-based measurements of EPP, but overestimates energy loss to the atmosphere.
2. Multibounce effects may be responsible for up to ~10% of the total number of electrons measured in the loss cone, and up to ~4% of electrons measured in the anti loss cone.
3. Particles energies of ~20 keV to 1 MeV and pitch angles within 20° of the loss cone edge have a higher likelihood of backscatter, indicating a 'sweet spot' of momenta where particles are likely to cause measurable multibounce effects for in-situ measurements.

4. General trends in predicted backscatter align with previous work – Cotts (2011)<sup>4</sup> predicts decreasing backscatter fraction with increasing energy above 100 keV and increasing backscatter fraction near the loss cone edge. Marshall (2018)<sup>5</sup> predicts the same general trends, but with more extreme effects (lower backscatter fractions deep in the loss cone and higher grazing fractions).

## Caveats

1. The G4EPP lookup tables have artifacts around 100 keV & 800 keV (Figure 6), work is ongoing to debug this issue.
2. G4EPP lookup tables operate on a fixed MLAT/magnetic field rotation angle, meaning they are not fully 1:1 with ELFIN data at some MLATs.
3. G4EPP backscatter number & energy measurements do not count secondaries.

## References

1. Berland, Marshall+ (2023), doi:10.1029/2023EA002987
2. Agostinelli, Allison+ (2003), doi:10.1016/S0168-9002(03)01368-8
3. Angelopoulos, Tsai+ (2020), doi:10.1007/s11214-020-00721-7
4. Cotts, Inan+ (2011), doi:10.1029/2011JA016581
5. Marshall, Bortnik, (2018), doi:10.1002/2017JA024873